RESEARCH   **Open Access**

CrossMark

Plasmonic behavior of III-V semiconductors in far-infrared and terahertz range

Jan Chochol[1,2]* , Kamil Postava[3], Michael Čada[2], Mathias Vanwolleghem[4], Martin Mičica[1,4],
Lukáš Halagačka[1,3], Jean-François Lampin[4] and Jaromír Pištora[1]

Abstract

Background: In this article, III-V semiconductors are proposed as materials for far-infrared and terahertz plasmonic applications. We suggest criteria to estimate appropriate spectral range for each material including tuning by fine doping and magnetic field.

Methods: Several single-crystal wafer samples (n,p-doped GaAs, n-doped InP, and n,p-doped and undoped InSb) are characterized using reflectivity measurement and their optical properties are described using the Drude-Lorentz model, including magneto-optical anisotropy.

Results: The optical parameters of III-V semiconductors are presented. Moreover, strong magnetic modulation of permittivity was demonstrated on the undoped InSb crystal wafer in the terahertz spectral range. Description of this effect is presented and the obtained parameters are compared with a Hall effect measurement.

Conclusion: Analyzing the phonon/free carrier contribution to the permittivity of the samples shows their possible use as plasmonic materials; the surface plasmon properties of semiconductors in the THz range resemble those of noble metals in the visible and near infrared range and their properties are tunable by either doping or magnetic field.

Keywords: Surface plasmons, Semiconductor materials, Magneto-optical materials, THz-TDS, FTIR

Background

Utilizing the terahertz range for better and faster communications [1–3], sensing [4], medicine [5] and security [6] has created a need for devices, capable of operating in the desired frequency range of 0.1-30 THz. One of the principles that can serve as the basis of guiding, coupling and modulating THz waves is the surface plasmon - an interface wave propagating at the boundary of negative (conductive) and positive (dielectric) permittivity material. Traditional plasmonic materials usable in visible/near infrared range, noble metals, are unsuitable for uses in the THz regime due to low confinement to the metal;

the wave is weakly bound to the interface, a phenomenon sometimes called the Zenneck plasmon [7]. Semiconductors with their carrier levels have their metallic properties shifted to lower frequencies - microwave, terahertz and far infrared. They are therefore suitable as building blocks for THz devices. Furthermore, they allow for much needed control of their electromagnetic properties. In the manufacturing the carrier levels can be adjusted by doping and after the manufacturing the properties can be controlled by light [8], temperature [9], electric gating [10] and by external magnetic field [11].

This paper compares plasmonic behavior of several samples of doped III-V semiconductors (InP-n, GaAs-n,p, InSb-n,p) and undoped InSb through spectroscopic characterization using a terahertz time-domain spectrometer (THz-TDS) in the range of 2–100 cm^{-1} and a Fourier transform infrared spectrometer (FTIR) in the range of 50–7500 cm^{-1}. Appropriate figures of merit are estimated to establish suitable ranges for room temperature

*Correspondence: jan.chochol@vsb.cz; jan.chochol@dal.ca;
jan.chochol@gmail.com
[1]Nanotechnology Centre, VSB – Technical University of Ostrava, 17. listopadu
15/2172, 708 33 Ostrava, Poruba, Czech Republic
[2]Department of Electrical and Computer Engineering, Dalhousie University,
6299 South St, Halifax NS B3H 4R2, Canada
Full list of author information is available at the end of the article

Chochol *et al. Journal of the European Optical Society-Rapid Publications* (2017) 13:13

Page 2 of 8

plasmonics applications. Furthermore, the undoped InSb sample is characterized in the presence of static magnetic field to explore the magnetic modulation.

The issue of semiconductor plasmonic properties in the far-infrared and terahertz range have been undertaken by several groups. The work of Palik and Furdyna [12] provides the necessary theory for optical and magneto-optical behavior of semiconductors. The experiments of Shubert et al. [13, 14] and Hofmann [15] show the potential of spectroscopic techniques in investigating that behavior, while further works [16–22] demonstrate the power of terahertz time-domain spectroscopy in determining the conductive and optical functions of semiconductors. Moreover, several papers [23–25] deal with the theory of the existence of surface plasmons in magnetically tunable materials.

Section "Optical functions of doped semiconductors" outlines the tools necessary for describing and modeling optical properties using the Drude-Lorentz model. Sections "Samples" and "Measurement" describe samples and the techniques used, and Section "Results and discussion" presents the measured spectra with the permittivity and parameters obtained from a reflectivity fit. Section "Semiconductors as plasmonic materials" discusses the suitability of these materials for plasmonic applications and Section "Magnetic modulation" provides data for magnetic modulation of plasmonic properties on undoped InSb.

Methods
Optical functions of doped semiconductors
The optical and conductive properties of III-V semiconductors in the far infrared and terahertz range are governed by three mechanisms, the free carrier absorption, lattice vibration and background permittivity, originating from high-frequency interband absorptions. These mechanisms are summarized in the Drude-Lorentz function, as

$$\varepsilon_r = \varepsilon_\infty - \underbrace{\frac{\omega_p^2}{\omega^2 + i\gamma_p\omega}}_{\varepsilon_D} + \underbrace{\frac{A_L\omega_L^2}{\omega_L^2 - \omega^2 - i\gamma_L\omega}}_{\varepsilon_L} , \quad (1)$$

which consists of three terms. The first one is the constant ε_∞, the background permittivity. The second one is the Drude term ε_D, originating from free carriers, where

$$\omega_p = \left(\frac{Ne^2}{\varepsilon_0 m^*}\right)^{\frac{1}{2}} \quad (2)$$

is the plasma frequency, N is the carrier concentration, e is the electron charge, ε_0 is the permittivity of free space and m^* is the effective mass of the charge carriers. γ_p is the damping constant, the inverse of the scattering time $\tau_p = 1/\gamma_p$.

The last term is the Lorentz term ε_L, describing a lattice vibration at the frequency ω_L, with the damping constant $\gamma_L = 1/\tau_L$ and the amplitude A_L. The amplitude can be understood as the difference between the permittivity limit below and above the oscillation at ω_L.

The parameters ε_∞, ω_p, τ_p, ω_L, τ_L, and A_L are the fitting parameters for the Drude-Lorentz model. The measured quantity is the reflectivity R, modeled using Berreman 4×4 matrix method [26].

The measurement of reflectivity allows us to obtain only the plasma frequency and the scattering time, in addition to the constant term and parameters of the Lorentz oscillator, as defined by Eq. (1). Using the plasma frequency and scattering time one can calculate the DC conductivity as

$$\sigma_0 = \frac{Ne^2\tau}{m^*} = \varepsilon_0 \omega_p^2 \tau . \quad (3)$$

Samples
We have measured six representative samples of single-crystal III-V semiconductors. All were polished on one side.

The GaAs samples were 2", 0.35 mm thick wafers made by AXT, Inc. One n-doped with Si dopants, with the reported electron concentration of $(0.8 - 4) \times 10^{18}$ cm^{-3} and the mobility of $(1 - 2.5) \times 10^3$ cm^2/Vs. One p-doped (Zn), with the reported hole concentration of $(0.5 - 5) \times 10^{19}$ cm^{-3} and the mobility of $50 - 120$ cm^2/Vs.

The InP sample was 2", 0.35 mm thick wafer also from AXT. It is n-doped with Sulfur; manufacturer reports values of $N = (0.8 - 8) \cdot 10^{18}$cm^{-3} and $\mu = (1 - 2.5) \cdot 10^3$cm^2/Vs.

Measured samples of InSb are n-doped (Te), p-doped (Ge) and undoped. All InSb samples were manufactured by MTI Corp as wafers of 2" diameter and a small square 10x10 mm of undoped InSb. The small sample was used for the Hall measurements by 4-contact van der Pauw method. The thickness of the wafers was 0.5 mm for the n-doped and 0.45 mm for the undoped and p-doped. The small sample has thickness of 0.45 mm. The n-doped samples have the manufacturer's reported carrier concentration of $(0.19 - 0.50) \cdot 10^{18}$ cm^{-3} and the mobility of $(3.58 - 5.60) \cdot 10^4$ cm^2/Vs, both at 77 K. The p-doped samples have the following reported parameters: $N = 0.5 - 5 \cdot 10^{17}$ cm^{-3} and $\mu = 4 - 8.4 \cdot 10^3$ cm^2/Vs, again at 77 K.

Measurement
We used two spectrometers to characterize the samples. The first one is the terahertz time-domain spectrometer TPS Spectra 3000 from TeraView Co., measuring in the THz range of 2-100 cm^{-1}. The second one is the Fourier transform infrared spectrometer Bruker Vertex

70v, measuring in the far-infrared range of 50–680 cm^{-1} and in the mid-IR range of 370–7500 cm^{-1}. All measurements were done in reflection configuration, with a fixed angle of incidence of 11 degrees, which doesn't allow measurements at smaller angles due to space limitations. On the other hand, such angle of incidence can be considered as near normal one and simplifies description of reflective phenomena. The data in overlapping ranges were averaged. We have used a thick gold layer as the reference. To avoid the influence of water vapor absorption, both reflection spectra were measured in vacuum.

Results and discussion

Spectroscopic characterization

Figure 1 shows the reflectivity spectra and the permittivity of the samples with the resulting parameters listed in Table 1 and the obtained permittivity in Fig. 2.

The sharp minima in reflectivity between 150 and 300 cm^{-1} corresponds to a crossing of the real part of the permittivity with the permittivity of vacuum due to the lattice vibrations. The fitted value of the Lorentz oscillator frequency is at the maximum of the imaginary part of the permittivity, called the transversal phonon [27]. The Lattice vibrations match those reported by other authors (InP [28], GaAs [11], InSb [12]).

The plasma edge, a region where the real part of the permittivity crosses zero and becomes negative for lower frequencies due to the free carries and the reflectivity rises is tied to the concentration and effective mass. For metals described by the Drude term, this would be where $\Re\{\varepsilon\} = 0$. Semiconductors however have a strong background permittivity, which from Eq. (1), places the

crossover frequency (reduced plasma freq.) between positive and negative at $\omega = \omega_p/\sqrt{\varepsilon_\infty}$ and the reflectivity minimum at $\omega = \omega_p/\sqrt{\varepsilon_\infty - 1}$; assuming no damping and negligible effect of the phonon. Real cases show effect of the phonon and damping, i.e. the n-doped GaAs the reflectivity minimum would be at 545.2 cm^{-1} but the real one is at 573.6 cm^{-1}. The effect of damping is strongly present in the p-doped samples, where the short scattering time of the holes makes the reflectivity spectra much shallower.

Semiconductors as plasmonic materials

There are two basic formulae describing the behavior of surface plasmon polaritons (SPP) on an interface between a dielectric and a metal/semiconductor. Those are the expressions for the wave vector components along the interface (y direction) and perpendicular to it (z direction). With the wave vector defined as $\mathbf{k} = \mathbf{x}k_x + \mathbf{y}k_y + \mathbf{z}k_z$ and assuming $k_x = 0$, the components of interest are

$$k_y = \frac{\omega}{c}\sqrt{\frac{\varepsilon_1\varepsilon_2}{\varepsilon_1 + \varepsilon_2}} , \qquad (4a)$$

$$k_{zj} = \frac{\omega}{c}\sqrt{\frac{\varepsilon_j^2}{\varepsilon_1 + \varepsilon_2}} , \qquad (4b)$$

where $j = 1, 2$ is the index of the respective media. For simplicity, let us assume the top medium is air, $\varepsilon_1 = 1$. To ensure a propagating surface plasmon polariton, two conditions must be fulfilled. The k_y (component along the interface) must be real and k_{zj} must be imaginary to ensure the localization of the plasmon (assuming just real permittivities). This occurs when the real part of ε_2 is negative
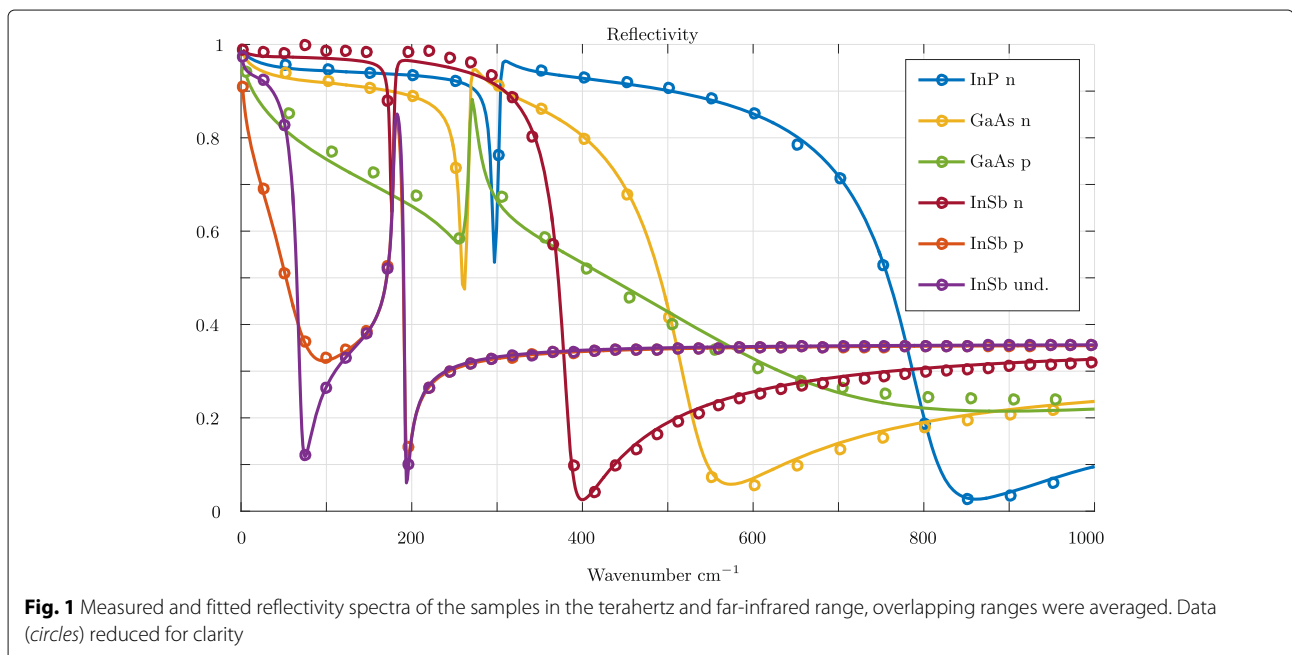

Fig. 1 Measured and fitted reflectivity spectra of the samples in the terahertz and far-infrared range, overlapping ranges were averaged. Data (*circles*) reduced for clarity

Chochol *et al. Journal of the European Optical Society-Rapid Publications* (2017) 13:13

Page 4 of 8

Table 1 Fitted parameters of GaAs, InP and InSb

	GaAs n-doped	GaAs p-doped	InP n-doped	InSb n-doped	InSb p-doped	InSb undoped
ω_p (10^{14} rad/s)	3.33 ± 0.01	4.44 ± 0.02	4.70 ± 0.01	2.82 ± 0.01	0.63 ± 0.01	0.57 ± 0.01
ω_p (cm^{-1})	1769.2 ± 1.9	2356.4 ± 9.1	2494.1 ± 1.8	1495.2 ± 1.83	332.6 ± 1.49	302.4 ± 0.33
τ_p (10^{-1} ps)	0.71 ± 0.01	0.09 ± 0.01	0.71 ± 0.01	2.65 ± 0.04	0.75 ± 0.01	5.16 ± 0.06
ω_L (10^{13} rad/s)	5.06 ± 0.01	5.06 ± 0.01	5.73 ± 0.01	3.38 ± 0.01	3.38 ± 0.01	3.38 ± 0.01
ω_L (cm^{-1})	268.4 ± 0.1	268.5 ± 0.2	303.9 ± 0.1	179.4 ± 0.13	179.4 ± 0.06	179.5 ± 0.06
τ_L (ps)	2.79 ± 0.27	1.95 ± 0.29	3.01 ± 0.24	1.81 ± 0.13	1.90 ± 0.04	1.99 ± 0.04
A_L	2.13 ± 0.03	2.15 ± 0.09	2.89 ± 0.04	2.02 ± 0.07	2.00 ± 0.01	2.02 ± 0.01
ε_∞	11.58 ± 0.01	11.34 ± 0.02	10.01 ± 0.01	15.68 ± 0.03	15.74 ± 0.01	15.86 ± 0.01
σ_0 (kS/m)	69.46 ± 0.54	16.54 ± 0.22	139.06 ± 0.77	186.35 ± 2.63	2.51 ± 0.04	14.83 ± 0.17

and is greater in absolute value than that of ε_1, which must be positive. That means $\Re\{\varepsilon_2\} < -\varepsilon_1$. A real case scenario has both components complex, meaning that the surface plasmon is decaying with propagation. The propagation length, denoted here as L_{SPP} when the electric field of the SPP drops to $1/e$ is simply $L_{SPP} = 1/\Im\{k_y\}$ and the penetration into the material (again, when the field drops to $1/e$) is $L_{1,2} = 1/\Im\{k_{z1,2}\}$.

An ideal material would allow a long propagation length of the SPP along the interface, yet sufficient confinement into the metallic (conductive) material; in other words short extension into the dielectric. When the difference between the permittivities ε_1 and ε_2 is large, the SPP can propagate many wavelengths, but is poorly guided by the interface (a small penetration depth into the conductor) and most of its energy is carried in the dielectric. The opposite is also valid - a heavily confined wave will have a lot of energy traveling in the absorbing material, and thus the propagation length is short.

Noble metals such as gold or silver are used for plasmonic applications in the visible and near-infrared range. By comparing the properties of the SPP on gold in the visible range and on semiconductors in the THz range, one can estimate how suitable the semiconductors are for plasmonic applications in the THz range. The comparison of the propagation length (along the interface) and the penetration (into the conducting material) normalized to the free space wavelength of light is shown in Fig. 3.

As Fig. 3 shows, the properties of semiconductors in the THz are almost identical to that of gold and silver in the visible range. For longer wavelengths, the trends on noble metals continue linearly to smaller confinement and longer propagation. The semiconductors do have several advantages. The adjustable doping concentration can significantly change the behavior of semiconductor, as can be seen from comparing the three samples of InSb. Even the p-doped sample is shown to be able of sustaining a surface
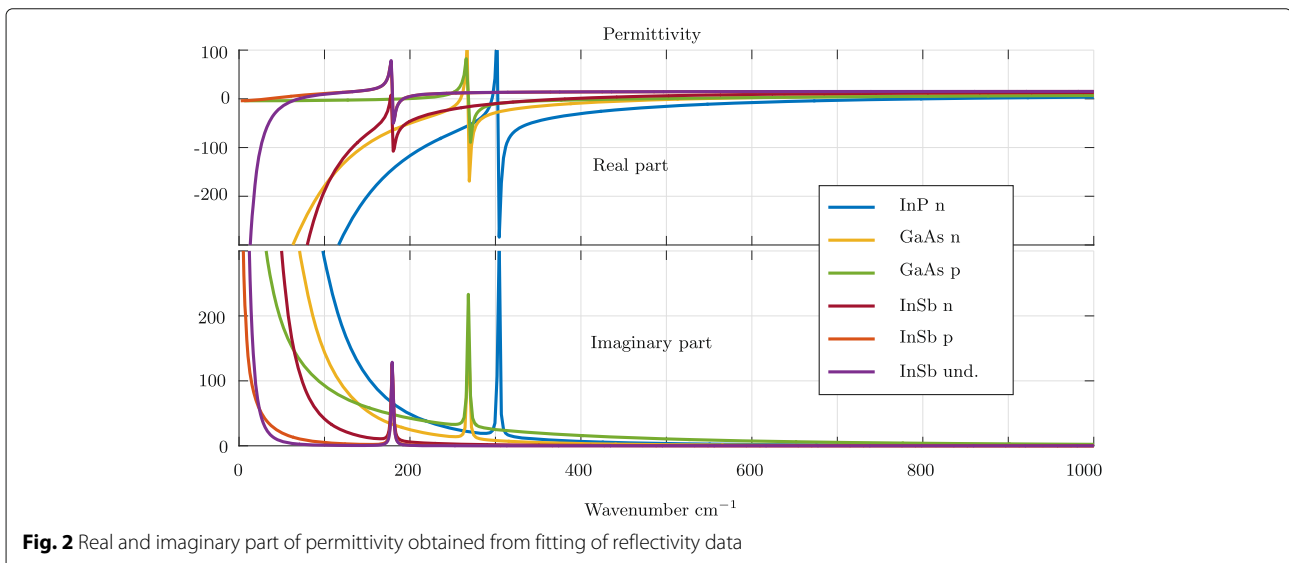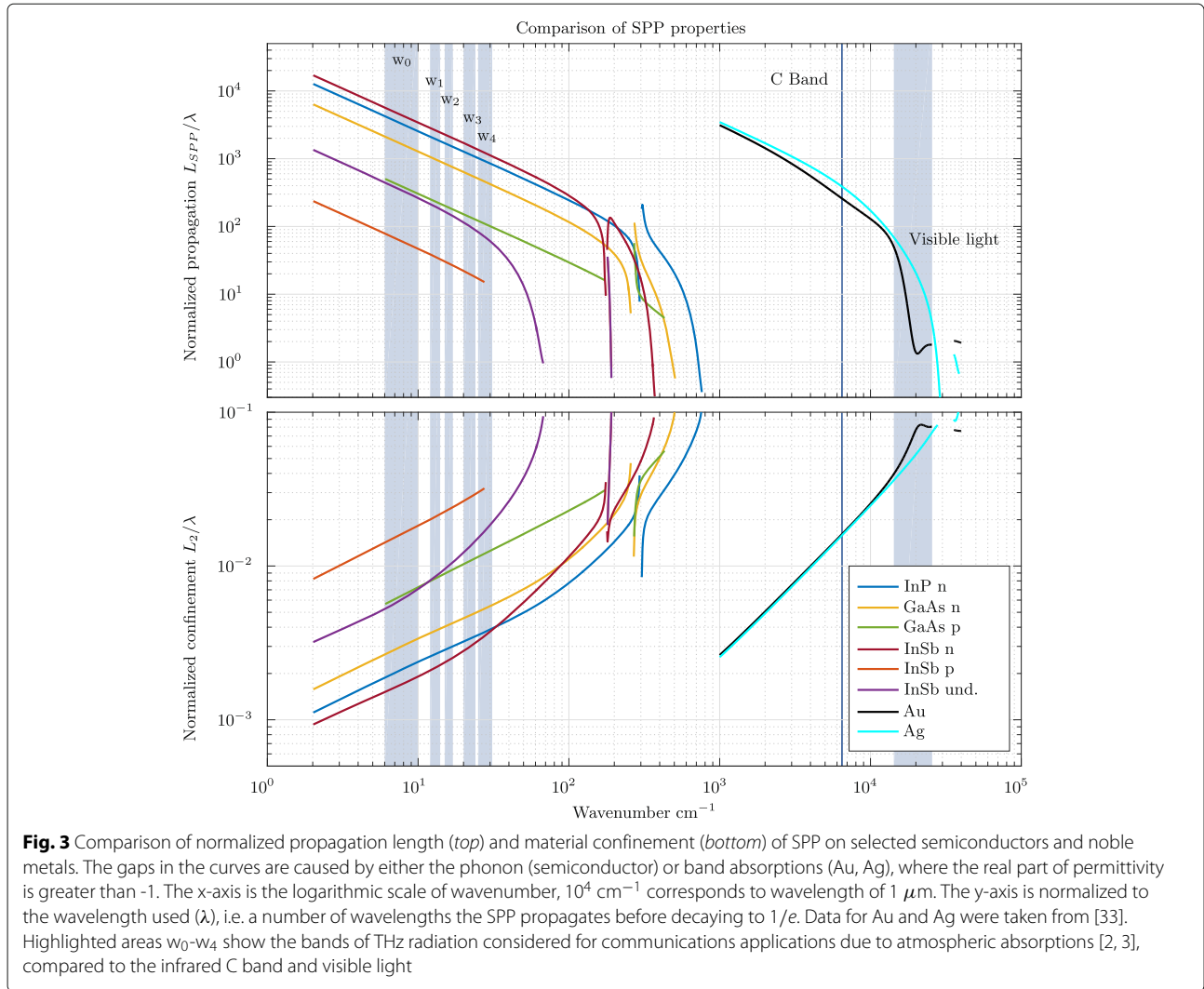
Fig. 2 Real and imaginary part of permittivity obtained from fitting of reflectivity data

Fig. 3 Comparison of normalized propagation length (*top*) and material confinement (*bottom*) of SPP on selected semiconductors and noble metals. The gaps in the curves are caused by either the phonon (semiconductor) or band absorptions (Au, Ag), where the real part of permittivity is greater than -1. The x-axis is the logarithmic scale of wavenumber, 10^4 cm^{-1} corresponds to wavelength of 1 μm. The y-axis is normalized to the wavelength used (λ), i.e. a number of wavelengths the SPP propagates before decaying to $1/e$. Data for Au and Ag were taken from [33]. Highlighted areas w$_0$-w$_4$ show the bands of THz radiation considered for communications applications due to atmospheric absorptions [2, 3], compared to the infrared C band and visible light

plasmon for low energies. Therefore, doping can be used to fine-tune the plasmonic properties of semiconductors. Other techniques, such as optical pumping, electric gating, or as demonstrated in the next section, magneto-optics allow for further tuning, switching or modulation of surface plasmons on semiconductors. The gaps in the curves, caused by the phonon, and the rapid change of behavior around them, lead to a surface phonon-polariton (i.e. on the undoped InSb) or a combination of both, where the electromagnetic energy is stored not just in the collective oscillation of the free carriers, but also in the vibrations of the lattice.

Magnetic modulation

This section uses a simple THz reflectivity measurement to demonstrate the strength of this magnetic modulation on undoped InSb. Similar experiment has been done by Ino [21] on InAs. This type of measurement has been called the "Optical Hall effect" [11].

In the presence of the magnetic field the permittivity tensor becomes anisotropic. In our case, the magnetic field is in the *z*-direction (perpendicular to the interface in the *x* and *y* directions, $y - z$ is the plane of incidence). A derivation is presented in the [27]. The form of the tensor with the magnetic field applied in the *z* direction (polar configuration) is

$$\hat{\varepsilon}_r = \begin{bmatrix} \varepsilon_{xx} & \varepsilon_{xy} & 0 \\ \varepsilon_{yx} & \varepsilon_{yy} & 0 \\ 0 & 0 & \varepsilon_{zz} \end{bmatrix}. \tag{5}$$

The *zz* component stays the same as ε_r in (1) and *xx*, *yy*, *xy*, *yx* components of the Drude term (shown with the constant term) change to

$$\varepsilon_{D,xx} = \varepsilon_{D,yy} = \varepsilon_\infty - \frac{\omega_p^2(\omega^2 + i\gamma_p\omega)}{(\omega^2 + i\gamma_p\omega)^2 - \omega_c^2\omega^2}, \tag{6a}$$

$$\varepsilon_{D,xy} = -\varepsilon_{D,yx} = -i\frac{\omega_p^2\omega_c\omega}{(\omega^2 + i\gamma_p\omega)^2 - \omega_c^2\omega^2}, \tag{6b}$$

Chochol *et al. Journal of the European Optical Society-Rapid Publications* (2017) 13:13

Page 6 of 8

which contain an additional fitting parameter, proportional to the magnetic induction, the cyclotron frequency, defined as

$$\omega_c = \frac{eB}{m^*}. \tag{7}$$

The Lorentz term can also be affected by the magnetic field, however the oscillations correspond to lattice vibrations, with much heavier particles than free electrons with an effective mass of $\sim 0.02\, m_0$. No effect has been observed in GaAs at 8 T [11]. It is thus appropriate to neglect the effect of the magnetic field for the Lorentz term.

For measurements with the magnetic field, a small permanent magnet was placed on the backside of the sample. The magnet creates a magnetic field of 0.43T, which was measured by a Gaussmeter. Variable field was obtained using plastic spacers. One wire grid on polyethylene polarizer was used as both polarizer and analyzer (TE polarization). The phase information comes from three parts, $\varphi = \varphi_{\text{sample}} - \varphi_{\text{reference}} - \varphi_{\text{shift}}$. φ_{sample} is the phase angle of the complex reflection coefficient of the sample and φ_{shift} stems from the misalignment d of the sample and reference, as $\varphi_{\text{shift}} = 4\pi d \cos \alpha_i / \lambda$. The φ_{shift} is a fitting parameter in the data treatment (d is on the order of $1–100\,\mu m$) and is subtracted from the data for plotting.

The obtained parameters were verified using Hall effect [29] measurement - a standard Van der Pauw (VdP) measurement [30]. A good ohmic contact was obtained by placing the probes on the sample, so there was no need for soldering.

The bottom graph in Fig. 4 is the reflectivity and phase measured with the applied magnetic field 0.43 T and 0.29 T (nominal value 0.23 T due to the effect of spacer), and it shows a clear change in the TE reflectivity caused by the magnetically induced anisotropy. The fitting was done simultaneously with the results without magnetic

field, so that the only difference is the cyclotron frequency and phase shift. The corresponding cyclotron frequency for 0.43 T is 4.4×10^{12} rad/s (23.4 cm^{-1}). Figure 5 shows the model of modulated permittivities with parameters obtained from this measurement. The change in the permittivity ε_{xx} is very responsive to the magnetic field and it is possible to change sign for lower frequencies even using small field. The ε_{xy} components also rapidly change with the strength of applied magnetic field and interestingly exhibit maximum for certain magnetic field.

In the metric of magneto-optics [31], the polar Kerr rotation is 26.1 degrees at its maximum is at 81 cm^{-1} for the field 0.43 T. Knowing the cyclotron frequency and magnetic field lets us calculate the effective mass as $m^* = 0.0169m_0$, which is higher than the nominal value due to higher concentration of electrons due to thermal excitation. With the knowledge of effective mass, we can calculate the mobility $\mu = \frac{e\tau}{m^*}$, concentration $N = \frac{\omega_p^2 \varepsilon_0 m^*}{e^2} = \frac{\omega_p^2}{\omega_c} \frac{\varepsilon_0 B}{e}$ and Hall coefficient $R_H = -\frac{1}{Ne} = -\frac{\mu}{\sigma_0}$. The parameters are listed in Table 2. The differences in values obtained from electrical and spectroscopic measurement are due to different sensitivity of the measuring techniques to different mechanisms and their systematic errors. Generally, the electric VdP measurement is used with lithographically etched pattern, but if there is a good ohmic contact, it is possible to measure without it by placing the contact probes on to the sample. This measurement, used in our case, is prone to error due to possible misalignment of the contact probes. Moreover, the spectral characterization is sensitive only to the carriers with the highest plasma frequency, whereas VdP includes the effect of both. These effects combined explain the differences in obtained values. For measurement with higher doping levels see [32].
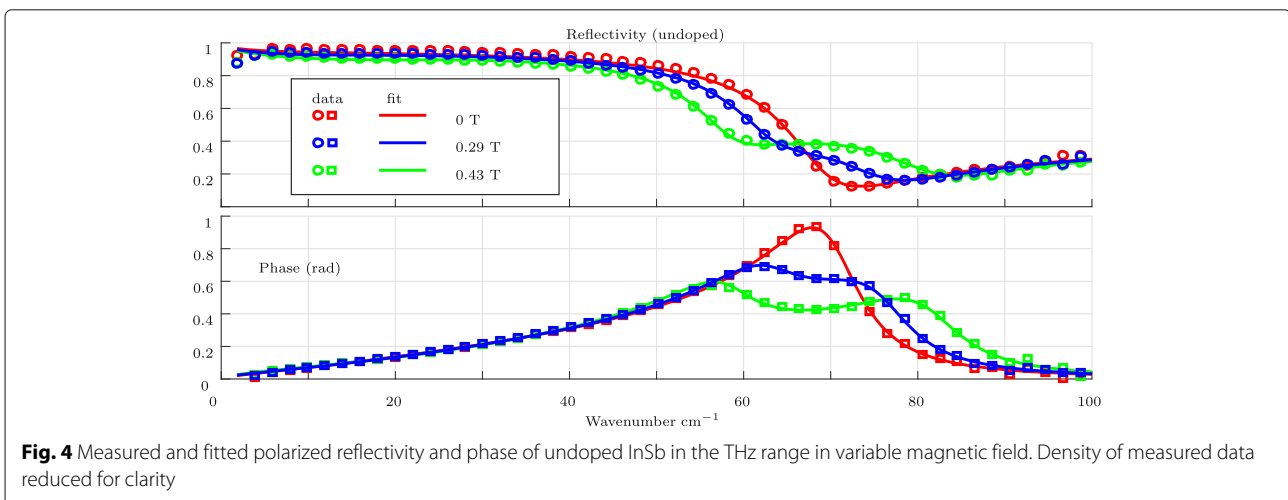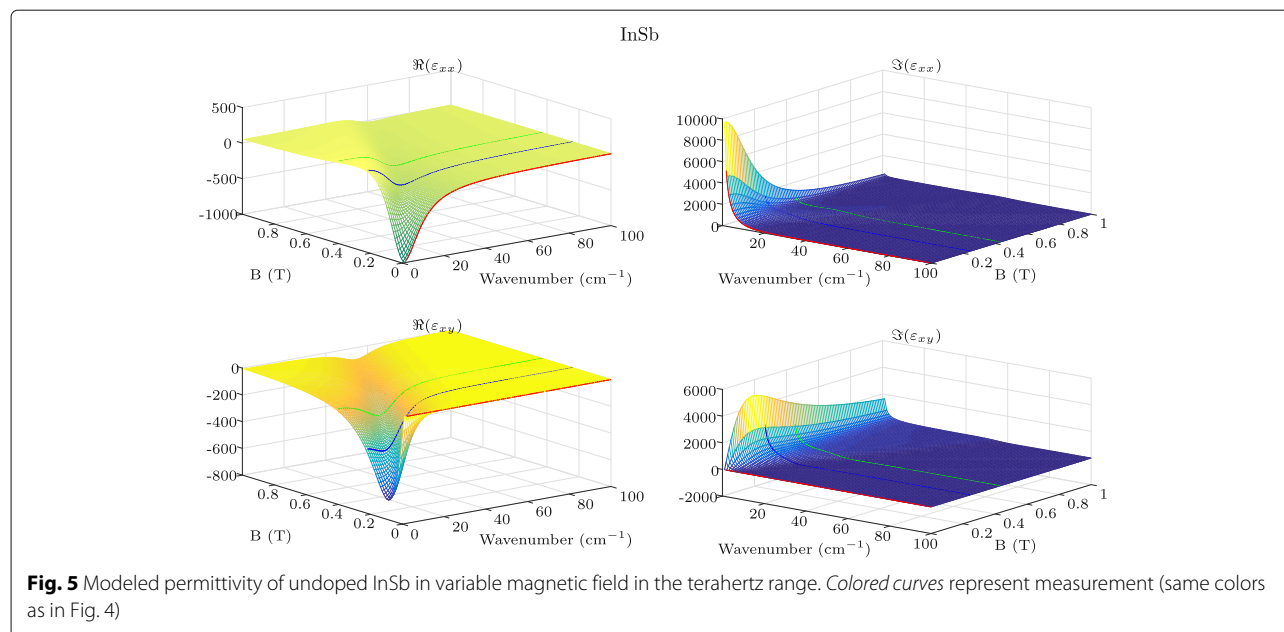

Fig. 4 Measured and fitted polarized reflectivity and phase of undoped InSb in the THz range in variable magnetic field. Density of measured data reduced for clarity

Chochol *et al. Journal of the European Optical Society-Rapid Publications* (2017) 13:13

Page 7 of 8

Fig. 5 Modeled permittivity of undoped InSb in variable magnetic field in the terahertz range. *Colored curves* represent measurement (same colors as in Fig. 4)

Conclusion

We have shown that the Drude-Lorentz model describes the optical properties of III-V semiconductors well. The THz-TDS and FTIR are suitable techniques for exploring properties of semiconductors in their respective ranges. The doping or intrinsic concentrations of free carriers in the measured ranges lead to a metal-like behavior. A surface plasmon polariton guided by these materials exhibits reasonable confinement and propagation length, similar to SPPs on noble metal-dielectric interface in the visible range. Thus semiconductors are suitable for the surface plasmon applications in the terahertz and far IR regime. An interesting property emerges with an applied magnetic field - a large anisotropy is induced, causing a huge magneto-optical effect. That can be used to significantly modulate the optical and guided wave properties using small magnetic field at room temperature. Free carrier magneto-optical effect is extremely weak in metals, due to their large plasma frequency and high effective mass and thus low cyclotron frequency. Coupled with low confinement of surface waves for THz frequencies in metals make semiconductors much more suitable for terahertz plasmonics.

Availability of data and materials
The data supporting the conclusions of this article are included within the present article.

Authors' contributions
JC conducted the experiments and engaged in writing, KP engaged in the experiments and writing, MC provided samples and expert advice, MV provided expert advice and writing, MM engaged in the experiments, LH engaged in modeling, JL engaged in the experiment design, JP contributed to writing and coordinated the work. All the authors have read and approved the final manuscript.

Competing interests
The authors declare that they have no competing interests.

Publisher's Note
Springer Nature remains neutral with regard to jurisdictional claims in published maps and institutional affiliations.

Author details
[1]Nanotechnology Centre, VSB – Technical University of Ostrava, 17. listopadu 15/2172, 708 33 Ostrava, Poruba, Czech Republic. [2]Department of Electrical and Computer Engineering, Dalhousie University, 6299 South St, Halifax NS B3H 4R2, Canada. [3]Department of Physics, VSB – Technical University of

Table 2 Comparison of parameters of undoped InSb, measured by Van der Pauw method and by spectral reflectivity measurement. The effective mass estimated from the cyclotron frequency as $0.0169 \pm 0.0001\ m_0$

Measurement	Hall	Spectral
N ($10^{16} \mathrm{cm}^{-3}$)	2.03	1.78 ± 0.01
μ ($10^4\ \mathrm{cm}^2/\mathrm{Vs}$)	6.66	5.76 ± 0.03
σ_0 (kS/m)	21.7	16.4 ± 0.07
R_H ($10^{-4}\ \mathrm{m}^3/\mathrm{C}$)	-3.07	-3.51 ± 0.02

Chochol *et al. Journal of the European Optical Society-Rapid Publications* (2017) 13:13

Page 8 of 8

Ostrava, 17. listopadu 15/2172, 708 33 Ostrava, Poruba, Czech Republic.
[4]Institut d'Electronique, de Microélectronique et de Nanotechnologie, UMR CNRS 8520, Avenue Poincaré, F-59652 Villeneuve d'Ascq cedex, France.

References

1. Nagatsuma, T, Ducournau, G, Renaud, CC: Advances in terahertz communications accelerated by photonics. Nat. Photonics. **10**, 371–379 (2016)
2. Akyildiz, IF, Jornet, JM, Han, C: Terahertz band: Next frontier for wireless communications. Phy. Com. **12**, 16–32 (2014)
3. Seeds, AJ, Shams, H, Fice, MJ, Renaud, CC: TeraHertz Photonics for Wireless Communications. J. Lightwave Technol. **33**, 579–587 (2015)
4. O'Hara, JF, Withayachumnankul, W, Al-Naib, I: A Review on Thin-film Sensing with Terahertz Waves. J. Infrared Millim. Te. **33**, 245–291 (2012)
5. Yang, X, Zhao, X, Yang, K, Liu, Y, Liu, Y, Fu, W, Luo, Y: Biomedical Applications of Terahertz Spectroscopy and Imaging. Trends Biotechnol. **34**, 810–824 (2016)
6. Liu, H-B, Zhong, H, Karpowicz, N, Chen, Y, Zhang, X-C: Terahertz Spectroscopy and Imaging for Defense and Security Applications. P. IEEE. **95**, 1514–1527 (2007)
7. Jeon, T-I, Grischkowsky, D: THz Zenneck surface wave (THz surface plasmon) propagation on a metal sheet. Appl. Phys. Lett. **88**, 061113 (2006)
8. Cooke, DG, Jepsen, PU: Optical modulation of terahertz pulses in a parallel plate waveguide. Opt. Express. **16**, 15123–15129 (2008)
9. Gómez Rivas, J, Kuttge, M, Kurz, H, Haring Bolivar, P, Sánchez-Gil, JA: Low-frequency active surface plasmon optics on semiconductors. Appl. Phys. Lett. **88**, 082106 (2006)
10. Rahm, M, Li, J-S, Padilla, WJ: THz Wave Modulators: A Brief Review on Different Modulation Techniques. J. Infrared Millim. Te. **34**, 1–27 (2013)
11. Kühne, P, Herzinger, CM, Schubert, M, Woollam, JA, Hofmann, T: Invited Article: An integrated mid-infrared, far-infrared, and terahertz optical Hall effect instrument, Vol. 85 (2014)
12. Palik, ED, Furdyna, JK: Infrared and microwave magnetoplasma effects in semiconductors. Rep. Prog. Phys. **33**, 1193 (1970)
13. Schubert, M, Hofmann, T, Herzinger, CM: Generalized far-infrared magneto-optic ellipsometry for semiconductor layer structures: determination of free-carrier effective-mass, mobility, and concentration parameters in n-type GaAs. J. Opt. Soc. Am. A. **20**, 347–356 (2003)
14. Schubert, M, Hofmann, T, Šik, J: Long-wavelength interface modes in semiconductor layer structures. Phys. Rev. **B 71** (2005)
15. Hofmann, T, Herzinger, CM, Krahmer, C, Streubel, K, Schubert, M: The optical Hall effect. Phys. Status Solidi A. **205**, 779–783 (2008)
16. Mittleman, DM, Cunningham, J, Nuss, MC, Geva, M: Noncontact semiconductor wafer characterization with the terahertz Hall effect. Appl. Phys. Lett. **71**, 16 (1997)
17. Kadlec, F, Kadlec, C, Kužel, P: Contrast in terahertz conductivity of phase-change materials. Solid State Commun. **152**, 852–855 (2012)
18. Kužel, P, Němec, H: Terahertz conductivity in nanoscaled systems: effective medium theory aspects. J. Phys. D Appl. Phys. **47**, 374005 (2014)
19. Jeon, T-I, Grischkowsky, D: Characterization of optically dense, doped semiconductors by reflection THz time domain spectroscopy. Appl. Phys. Lett. **72**, 3032 (1998)
20. Grischkowsky, D, Keiding, S, Van Exter, M, Fattinger, C: Far-infrared time-domain spectroscopy with terahertz beams of dielectrics and semiconductors. J. Opt. Soc. Am. B. **7**, 2006–2015 (1990)
21. Ino, Y, Shimano, R, Svirko, Y, Kuwata-Gonokami, M: Terahertz time domain magneto-optical ellipsometry in reflection geometry. Phys. Rev. **B 70**(15) (2004). https://doi.org/10.1103/PhysRevB.70.155101
22. Stanislavchuk, TN, Kang, TD, Rogers, PD, Standard, EC, Basistyy, R, Kotelyanskii, AM, Nita, G, Zhou, T, Carr, GL, Kotelyanskii, M, et al.: Synchrotron radiation-based far-infrared spectroscopic ellipsometer with full Mueller-matrix capability. Rev. Sci. Instrum. **84**, 023901 (2013)
23. Palik, ED, Kaplan, R, Gammon, RW, Kaplan, H, Wallis, RF, Quinn, JJ: Coupled surface magnetoplasmon-optic-phonon polariton modes on InSb. Phys. Rev. B. **13**, 2497 (1976)
24. Brion, JJ, Wallis, RF, Hartstein, A, Burstein, E: Theory of Surface Magnetoplasmons in Semiconductors. Phys. Rev. Lett. **28**, 1455–1458 (1972)
25. Kushwaha, MS: Plasmons and magnetoplasmons in semiconductor heterostructures. Surf. Sci. Rep. **41**, 1–416 (2001)
26. Berreman, DW: Optics in stratified and anisotropic media: 4×4 -matrix formulation. J. Opt. Soc. Am. **62**, 502–510 (1972)
27. Yu, P, Cardona, M: Fundamentals of Semiconductor: Physics and Materials Properties. Springer, Berlin Heidelberg (2013)
28. Jamshidi, H, Parker, TJ: The far infrared optical properties of InP at 6 and 300 K. Int. J. Infrared Milli. **4**, 1037–1044 (1983)
29. Spitzer, WG, Fan, HY: Determination of optical constants and carrier effective mass of semiconductors. Phys. Rev. **106**, 882 (1957)
30. van der Pauw, L: A method of measuring specific resistivity and Hall effect of discs of arbitrary shape. Philips Res. Rep. **13**, 1–9 (1958)
31. Visnovsky, S: Optics in Magnetic Multilayers and Nanostructures (Optical Science and Engineering). CRC Press, Boca Raton (2006)
32. Chochol, J, Postava, K, Čada, M, Vanwolleghem, M, Halagačka, L, Lampin, J-F, Pištora, J: Magneto-optical properties of InSb for terahertz applications. AIP Adv. **6**, 115021 (2016)
33. Rakić, AD, Djurišić, AB, Elazar, JM, Majewski, ML: Optical properties of metallic films for vertical-cavity optoelectronic devices. Appl. Opt. **37**, 5271–5283 (1998)